Cooperative Spin Crossover above Room Temperature in Iron(II) Cyanoborohydride Pyrazine Complex

Yurii S. Bibik[a], Sergiu Shova[b], Aurelian Rotaru[c], Sergii I. Shylin[d], Igor O. Fritsky[a], Rostyslav D. Lampeka[a], and Il'ya A. Gural'skiy [a*]

[a]*Department of Chemistry, Taras Shevchenko National University of Kyiv, 64 Volodymyrska St., 01601 Kyiv, Ukraine.*

[b] *"Petru Poni" Institute of Macromolecular Chemistry, Aleea Gr. Ghica Voda 41A, 700487 Iaşi, Romania*

[c]*Faculty of Electrical Engineering and Computer Science & MANSiD Research Center, Ştefan cel Mare University, Universitatii St. 13, 720229 Suceava, Romania*

[d]*Department of Chemistry – Ångström Laboratory, Uppsala University, Box 523, 75120 Uppsala, Sweden*

*Email: illia.guralskyi@univ.kiev.ua

ABSTRACT

Hysteretic spin crossover in coordination complexes of $3d$-metal ions represents one of the most spectacular phenomena of molecular bistability. In this paper we describe a self-assembly of pyrazine (pz) and $Fe(BH_3CN)_2$ that afforded a new 2D coordination polymer $[Fe(pz)_2(BH_3CN)_2]_\infty$. It undergoes an abrupt, hysteretic spin crossover (SCO) with $T_{1/2}$ of 338 K (heating) and 326 K (cooling) according to magnetic susceptibility measurements. Mössbauer spectroscopy revealed a complete transition between the low-spin (LS) and the high-spin (HS) states of the iron centers. This LS to HS transition induced an increase of the unit cell volume by 10.6%. Meanwhile, a modulation of multiple $[C- H^{\delta+} \cdots H^{\delta-}-B]$ dihydrogen bonds stimulates a contraction in direction c (2.2 %). Simplicity of the synthesis, mild temperatures of transition, a pronounced thermochromism, stability upon thermal cycling, a striking volume expansion upon SCO and an easy processability to composite films make this new complex an attractive material for switchable components of diverse applications.

INTRODUCTION

Spin crossover (SCO) is a well-known phenomenon of electronic reorganization in $3d$-metals compounds.[1] It is emerged from the existence of two electronic configurations, namely low-spin (LS, with a fewer number of unpaired electrons) and high-spin (HS, with a higher number of unpaired electrons). This phenomenon is also attracting attention because of a memory effect observed for some SCO systems and realized via appearance of a thermal hysteresis loop (when LS or HS configuration may exist at the same conditions, depending on the previous thermal history).[2]

Among different 3*d*-metal ions, Fe(II) takes leading positions as a central ion for engineering of SCO complexes. This is because there are many combinations of organic and inorganic ligands that are suitable for the construction of the switchable systems, and also practically attractive transition temperatures with a drastic change of many physical characteristics (optical, magnetic, electric, mechanical, etc.).

Unsubstituted pyrazine is a simple and a widely used bridging N,N'-donor ligand for the synthesis of Fe(II) SCO complexes. It is a notable building unit for constructing cyanometallic MOFs, so called analogues of Hofmann clathrates (with Ag, Au, Ni, Pd, Pt as co-metals).[3] They are 3D frameworks built of heterometallic cyano-bridged layers, that are interconnected by a pyrazine linker. They all display abrupt hysteretic SCO: Ag and Au above room temperature (RT),[3a,3b] Ni and Pt complexes near RT,[3c,3e] and Pd complex below RT.[3d] Some other pyrazine-based 3D frameworks with azide[4], thiocyanate[5] and 1,4-benzenedicarboxylic acid[6] as co-ligands are HS and do not display SCO. 2D grids built of Fe(II) ions bound with pyrazine linkers and supported with thiocyanate or selenocyanate anions as a co-ligand are also paramagnetic.[7] Meanwhile another ligand-mixed 2D framework (with pyrazine, *trans*-4,4'-azo-1,2,4-triazole and thiocyanate ligands) display a water-sensitive SCO below RT[8].

Pyrazine can also play a bridging role to form 1D chain coordination compounds. Known complexes are usually HS,[9] which is directly related to the presence of O-donor co-ligands in the coordination sphere of Fe(II). However, in case of selected co-ligands,[10] complexes can have incomplete (a Salen-type Schiff base co-ligand) or complete (acetonitrile co-ligand) SCO below RT. Worth noting, pyrazine based complexes with co-ligands can also serve as sensors and change their spin states via a single-crystal-to-single-crystal transformation[11] or desorption/absorption[12].

Cyanoborohydride (BH_3CN^-) is a small anionic N-donor ligand that has been successfully employed for the synthesis of molecular Fe(II) SCO complexes. The majority of these compounds contain two bidentate N-donor ligands forming the equatorial environment around Fe(II) centers and two BH_3CN^- anions in the *trans*-positions. Rodríguez-Jiménez et al.[13] have significantly contributed by synthesizing such complexes based on 4-(4-methylphenyl)-3-phenyl-5-(azine)-1,2,4-triazole, where azine = pyridine, 5-substitueted 2-pyridine, pyridazine, 4-pyrimidine, pyrazine, and 2-pyrimidine. All these complexes possess SCO in the solid state and in solutions, all below or near RT. The works of Scott, Ross et al.[14] are devoted to the complexes based on 2,2′-dipyridylamino-s-triazine core ligands, all with SCO. All mentioned BH_3CN^- complexes are formed by large rigid ligands that are capable to display π–π contacts and majorly crystallize with guest solvents that contribute to the SCO characteristics (cooperativity, temperature, completeness). Another family of molecular complexes is formed by tetradentate chelating ligands in *cis-α*-conformation and two BH_3CN^- co-ligands in *cis*-positions. Thus N,N'-bis(2-pyridylmethyl)-1,2-ethanediamine and its analogues can provide FeN_6[15] and FeN_4S_2[16] coordination environments. These complexes demonstrate a complete SCO in a wide range of temperatures; however, in case of large ligand molecules[15e,16b] a more distorted octahedral environment is formed and it inhibits the occurrence of SCO. Some other examples of molecular complexes with the BH_3CN^- co-ligand that do or do not display SCO can be found in references.[17]

BH$_3$CN$^-$ anion is also suitable for designing polymeric SCO complexes. They can be 1D helical chains,[18] 2D square grid networks,[19] or even 3D porous coordination polymers[20] when a tetradentate N,N'-bridging ligand is used. In the case when large aromatic ligands are employed, pores of various sizes can be achieved.

Notably, the works above evidence that in a series of compounds of a general formula $Fe(L)(XCN)_2$, where X = S, Se, BH_3, a borohydride derivative is more likely to possess SCO. Also, complexes containing BH_3CN^- usually have higher temperatures of SCO compared to their chalcocyanate counterparts.[15b,16b,21]

In this paper we report on a new Fe(II) coordination compound, which is a solvent-free 2D 4^4 grid network and is formed by pyrazine and BH_3CN^- ligands. Its crystal structure, magnetic, optical and calorimetric properties are studied and discussed.

EXPERIMENTAL SECTION

Materials. *p*-Toluenesulfonic acid monohydrate ($CH_3C_6H_4SO_3H \cdot H_2O$), iron powder (Fe), pyrazine (pz, $C_4H_4N_2$), sodium cyanoborohydride ($NaBH_3CN$) and ethanol were purchased from commercial sources and used as received. Iron(II) p-toluenesulphonate hexahydrate ($Fe(OTs)_2 \cdot 6H_2O$) was synthesized according to a previously reported procedure.[22]

Synthesis of Fe(pz)₂(BH₃CN)₂. An excess of $NaBH_3CN$ (100.5 mg, 1.6 mmol, 2 eq.) was dispersed in ethanol (5 ml) and mixed with a solution of $Fe(OTs)_2 \cdot 6H_2O$ (202.4 mg, 0.4 mmol, 1 eq.) in ethanol (1 ml). The obtained solution of $Fe(BH_3CN)_2$ was separated from a precipitate by centrifugation and an excess of pyrazine (192.3 mg, 2.4 mmol, 3 eq.) in ethanol (0.5 ml) was added under stirring. In 5 minutes, a formation of red crystals suitable for single crystal X-ray analysis was observed. In 1 hour, a dark red polycrystalline powder of $Fe(pz)_2(BH_3CN)_2$ was removed from the solution by centrifugation, washed with ethanol and dried in air. Yield is ca. 60.5 mg (51%). Anal. Calcd (%) for $C_{10}H_{14}B_2FeN_6$: C, 40.51; H, 4.73; N, 28.36. Found: C, 40.35; H, 4.79; N, 28.27. IR (cm^{-1}): 3106(w), 2332(m), 2200(m), 1600(w), 1474(w), 1412(s), 1186(m), 1168(m), 1118(s), 1048(m), 1016(w), 836(s), 762(w), 696(s).

Free standing films. A procedure similar to the described previously was applied. A powder of $Fe(pz)_2(BH_3CN)_2$ (4 mg) was dispersed in a solution of PMMA (16 mg, FW ~ 300) in $CHCl_3$ (0.25 ml) by stirring for 5 min. The suspensions were deposited on Teflon substrates at 35 °C and the chloroform was let to evaporate. After removing from the substrate, the annealing of films was done by heating at 95 °C for 1 h.

Physical Characterization.

X-ray diffraction. Single crystal XRD experiments for $Fe(pz)_2(BH_3CN)_2$ were made using Oxford-Diffraction XCALIBUR E CCD diffractometer with graphite-monochromated Mo-Kα radiation. Experiments were performed at 293 K. CrysAlisPro package from Oxford Diffraction was used to integrate the data and to determine the unit cell. The structures were solved with using intrinsic phasing methods (ShelXT program) and refined via least-squares minimization algorithm (ShelXL program).[23] Olex2 was used as a graphical interface for the solution and refinement of the structurs.[24] Non-hydrogen atoms were refined as anisotropic. Pyrazine molecule was refined as disordered between two positions (50:50). All hydrogen atoms were positioned geometrically and refined using a riding model (C-H = 0.93 Å, B-H = 1.08 Å). CCDC 2179860-2179861 contain the supplementary crystallographic data for this paper. These data can be obtained free of charge from The Cambridge Crystallographic Data Centre via www.ccdc.cam.ac.uk/data_request/cif. Crystallographic information for the LS structure of $Fe(pz)_2(BH_3CN)_2$ is summarized in Tables S1-S4.

PXRD measurements. PXRD was performed on Rigaku SmartLab 9kW diffractometer (Cu-Kα radiation) at 293 K (LS form) and 368 K (HS form) in the range of 2Θ 5 – 65° and a step of 0.005°. Refinement of the high-spin crystal structure was performed using Expo2014 software. Non-

hydrogen atoms were refined as isotropic. Bond lengths were restrained. Pyrazine molecule was refined as disordered between two positions (50:50). Crystallographic information for the high-spin structure of $Fe(pz)_2(BH_3CN)_2$ is summarized in Tables S5-S8.

Magnetic susceptibility measurements. Magnetic properties of $Fe(pz)_2(BH_3CN)_2$ as a function of temperature were studied in the range of 273–373 K using a MPMS3 SQUID magnetometer (Quantum Design Inc.), in DC mode (1000 Oe field). Cooling and heating rates were 2 K min^{-1}. Diamagnetic corrections of the sample holder and the complex (estimated from Pascal's constants) were applied.

Calorimetric measurements. DSC curves were obtained using Linkam DSC600 stage (N_2 environment, 10 K min^{-1} scan rate).

Optical reflectance measurements. Optical monitoring of SCO was performed using the an Optica SZM-1 microscope and a Sigeta UCMOS 1300 camera. Temperature control was made using DSC600 Linkam cryostat (scan rate 2 K min^{-1}, 303 – 373 K temperature range, N_2 environment). Images were acquired using ToupView software (one image per degree) and processed using ImageJ software.

UV-Vis spectroscopy. Absorption spectra were recorded at 298 K and 368 K with Varian Cary® 50 UV-Vis spectrophotometer (190–1100 nm).

Elemental analysis and FTIR. CHN elemental analysis was performed with a Vario Micro Cube (Elementar) CHNOS elemental analyzer. FTIR spectra were recorded at 293 K using PerkinElmer spectrometer BX II equipped with ATR sampling accessory (4000–650 cm^{-1}).

Mössbauer spectroscopy. [57]Fe Mössbauer experiments at 293 and 353 K was made as described previously. Powder sample of $Fe(pz)_2(BH_3CN)_2$ (50 mg) was used. Isomer shifts are given relative to iron metal at room temperature.

RESULTS AND DISCUSSION

Structure description. The title complex in the form of red crystals is rapidly formed by a reaction of $Fe(BH_3CN)_2$ with pz in ethanolic medium. Crystal structure of $Fe(pz)_2(BH_3CN)_2$ was obtained at 293 K. This complex crystalizes in the tetragonal *I4/mmm* space group with two formula units $Fe(pz)_2(BH_3CN)_2$ per cell (Table 1). A fragment of its structure illustrating a coordination environment of iron (II) is shown in Figure 1a. Iron(II) ion is located on a special position (Wyckoff position 2a); it has FeN_6 coordination environment of a slightly compressed octahedron that consists of two axial monodentate $NCBH_3^-$ anions and four equatorial nitrogen atoms from bridging pz ligands. At 293 K the average bond distance <Fe–N> for $Fe(pz)_2(BH_3CN)_2$ is equal to 1.981(2) Å, which correspond to its LS state.[25] All equatorial Fe–N bond lengths are the same and equal to 1.995(6) Å. Axial bonds are shorter and are equal to 1.952(4), probably because of a negative charge on the axial ligands, making them stronger σ-donors.

A pyrazine ligand can rotate around either *a* or *b* direction. This leads to its disorder between two positions in the structure obtained at room temperature (50:50) (Fig. 1c).

The resulting four-connected, planar structural unit leads to the formation of 2D grid-like layers in the *ab* plane with iron ions in the nodes and pz ligands as linkers. The 2D 4^4 square grid networks with sizes of 6.797 Å × 6.797 Å are stacked in the ABAB manner (Figure 2a,b), so that BH_3 groups point to the square holes of adjacent layers. Such kind of 2D Fe(II)-based SCO grids supported by

cyanoborohydride ions is known for much larger bridging N,N'-donor ligands, like 1,2-bis(4-pyridyl)ethane), 1,4-bis(pyrid-4-yl)benzene, 1,1,2,2-tetrakis(4-(pyridin-4-yl)phenyl)ethene.[19]

The major weak interactions responsible for staking 2D layers in a 3D supramolecular structure are C–H···H–B contacts (Figure 2c). These $H^{\delta-}$ to $H^{\delta+}$ contacts can be considered as an interaction between C–H proton and the B–H bond as a whole, and are known from literature as dihydrogen bonds[26]. They may play an important role in stabilization of a dense packing of 2D layers upon crystallization. In the title complex the H···H contacts are 2.076–2.254 Å, the B–H···H and C–H···H angles are 132.9–155.7° and 119.7–142.6°, respectively. These values are typical for C–$H^{\delta+}$···$H^{\delta-}$–B dihydrogen bonds,[19a] while one should consider that B–H and C–H bond lengths were fixed upon the refinement. A high disorder of H atoms of BH_3 group which is related to the high symmetry of the complex also contributes to the dispersion in the distances of H···H contacts. Usually, intermolecular interactions in SCO complexes are represented by hydrogen bonding[27] and π-π stacking[27b,28], while dihydrogen bonding is rare since SCO complexes lack metal hydride, borane type or similar fragments incorporating $H^{\delta-}$. In the title complex the presence of BH_3 groups stimulates the dihydrogen interactions that are responsible for stacking 2D layers in the ABAB manner, leading to the dense 3D supramolecular arrangement and ensuring no free space for any guest inclusion. Namely, the absence of guests is responsible for the stability of the SCO behavior, e.g., water guest effects are usually observed in complexes of such wide classes as 1,2,4-triazolic complexes[29] and analogues of Hofmann clathrates[30].

A comparison of the PXRD pattern of the polycrystalline sample obtained in the synthesis shows a nice agreement with the found crystal structure (Figure S2a). Unfortunately, upon heating single crystals to the temperatures where they are in HS state, they lose their quality and become unsuitable for X-ray analysis. PXRD patterns of the polycrystalline sample at 368 K show a

pronounceable change of the structure related to the LS→HS transition. Notably, a PXRD pattern recorded after 10 consequent thermal cycles shows the reversibility of the structural changes that occur in the complex upon the spin transition (Figure S2a). Indexing of the diffractogram reveals that the complex keeps its tetragonal symmetry in the HS state, while the unit cell increases by 10.6%. This change occurs because of expansions in a and b directions of 6.3% each. This is provoked by the Fe–N bond elongation that is typically observed upon a LS→HS transition (ca. 0.2 Å for Fe(II)). The pyrazine ligands are rigid and this strain is efficiently transmitted to the 4^4 nets. A less typically contraction of 2.2% occurs in c direction. Even though Fe to $NCBH_3$ distance also increases, the expansion of grid size to 7.229 Å × 7.229 Å leads to some changes the geometry of H···H contacts and allows a denser packing of 2D layers along the c direction (8.04 Å in LS state vs. 7.86 Å in HS state). Rietveld refinement of the HS structure (Figure S2b) reveals a satisfactory model with principal structural parameters summarized in Table 1.

Volume expansion always accompanies spin crossover in transition metal complexes. While the typical Fe–N bond length change is ~ 0.2 A (~10%), the total volume expansion is defined by the presence of bulky organic ligands the size of which remains unchanged. Labile fragments/contacts geometry of which can be adjusted upon the transition also affect the total expansion. Usually the expansion is within 2-10% range, e.g. for a similar complex with a longer bridging ligand an expansion of 5.5% is observed [19a]. Worth noting some exceptional examples with small ligands when the expansion reaches values above that in the title compound[31].
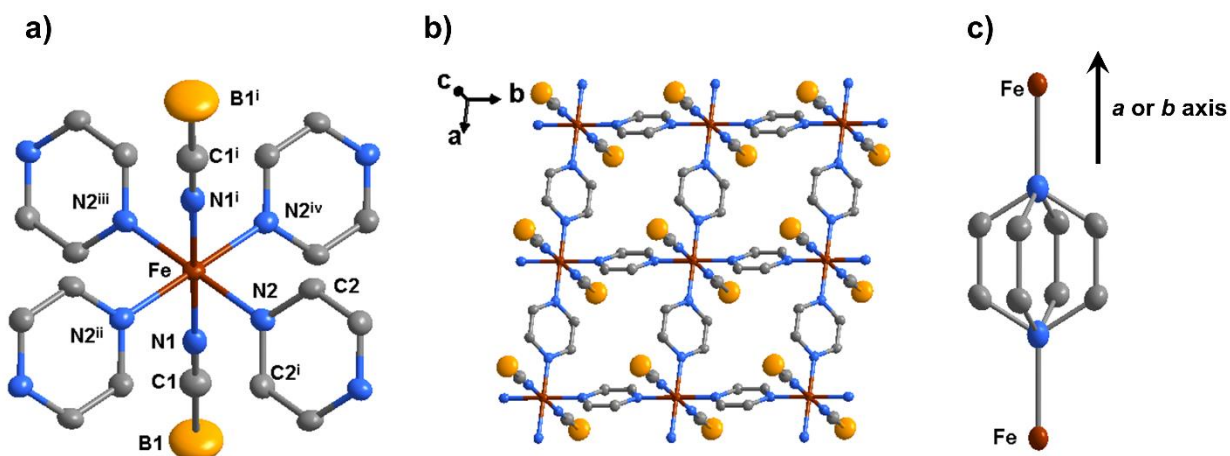
Figure 1. (a) Fragment of the crystal structure of $Fe(pz)_2(BH_3CN)_2$ showing atom labelling scheme. Displacement ellipsoids are shown with 50% probability. Symmetry codes: (i) *+x, 1-y, 1-z*; (ii) *+y, 1-x, +z*; (iii) *1-x, 1-y, 1-z*; (iv) *1-y, +x, +z*; (b) View of the crystal structure of $Fe(pz)_2(BH_3CN)_2$ demonstrating an infinite 2D layer; (c) Fragment of the crystal structure showing the pyrazine disorder along *a* or *b* axis.

Table 1. Selected structural parameters of $Fe(pz)_2(BH_3CN)_2$ in LS and HS forms

Parameter	LS (293 K)	HS (368 K)
a (Å)	6.797(3)	7.229(2)
b (Å)	6.797(3)	7.229(2)
c (Å)	16.082(5)	15.717(2)
V (Å^3)	743.0(7)	821.366(6)
Fe–N1 (Å)	1.952(4)	2.146(4)*
Fe–N2 (Å)	1.995(6)	2.176(4)*
<Fe–N> (Å)	1.981(2)	2.166(4)
V_{oct} [FeN$_6$] (Å^3)	10.367	13.562
ζ (Å)	0.115	0.080

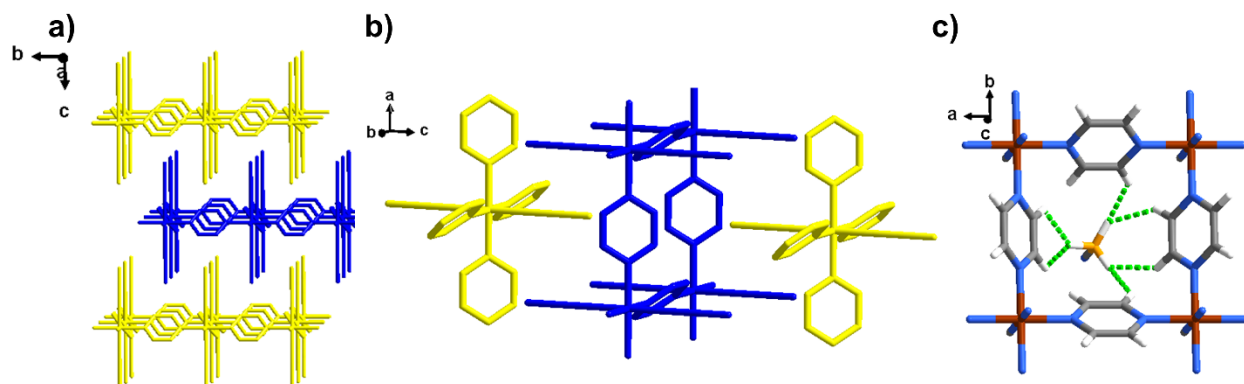| B···C (Å)	3.7386	3.7190

* parameters were restrained during the Rietveld refinement

Figure 2. (a, b) Interposition of the 2D grid-like layers of $Fe(pz)_2(BH_3CN)_2$ shown in blue and yellow; (c) Fragment of the crystal structure showing H···H contacts as dashed green lines.

Spin-crossover behavior. Temperature dependence of the magnetic susceptibility recorded on $Fe(pz)_2(BH_3CN)_2$ powder upon heating/cooling in the range 273 – 373 K is given in Figure 3. At room temperature the $\chi_M T$ value is 0.20 cm³ K mol⁻¹ which is attributed to the Fe(II) ion in the LS state (S = 0). Non-zero values of $\chi_M T$ at low temperatures may be explained by an inaccurate integration of the signal from a small amount of the diamagnetic sample (as described below, a Mössbauer spectrum of the complex evidences that there is no any residual HS fraction at low temperatures). The value of $\chi_M T$ remains almost constant upon heating to 334 K. Upon further heating $\chi_M T$ increases abruptly with $T_{1/2}\uparrow$ = 338 K attaining a value of 3.57 cm³ K mol⁻¹ at 373 K indicating that the transition to the HS state (S = 2) is practically completed. The subsequent cooling mode provides evidence for a 12 K hysteresis loop with $T_{1/2}\downarrow$ = 326 K. The spin transition is reproducible in the consequent thermal cycle, as seen from a good superpositions of the two transition loops (Figure 3). Such kind of abrupt transition above room temperature is not frequent

and mostly takes place in the complexes of Fe(II) with 4-substituted 1,2,4-triazoles[32] and analogues of Hofmann clathrates.[33] These spin transitions are among the most looked for since they occur at technologically important temperatures and possess a memory channel brought by a hysteresis loop.

The cooperativity of the transition is usually confirmed by its abruptness and the presence of the hysteresis loop. A quantitative criterion for that cooperativity is the parameter of cooperativity (Γ), which is introduced by the Slichter-Drickamer model[34]:

$$\ln \frac{(1-\gamma_{HS})}{\gamma_{HS}} = \frac{\Delta H + \Gamma(1-2\gamma_{HS})}{RT} - \frac{\Delta S}{R} \qquad (1)$$

where γ_{HS} is the HS fraction, R is the gas constant, ΔH is the enthalpy change, ΔS is the entropy change associated with the spin transition (thermodynamic parameters of SCO were extracted from DSC measurement described here below). A modeled curve is shown in Figure 3 and corresponds to $\Gamma = 6.6$ kJ mol^{-1}, that points on a high cooperativity of the spin transition compared with $2RT_{1/2}$ = 5.6 kJ mol^{-1} [35].

Notably, the closest structural analogues of the title complex which contain SCN$^-$ or SeCN$^-$ co-ligands do not have SCO,[7] in line with the general trend to more likely have SCO with BH$_3$CN$^-$ compared with SCN$^-$ and SeCN$^-$, regardless of the crystal packing and the nature of N-ligand.
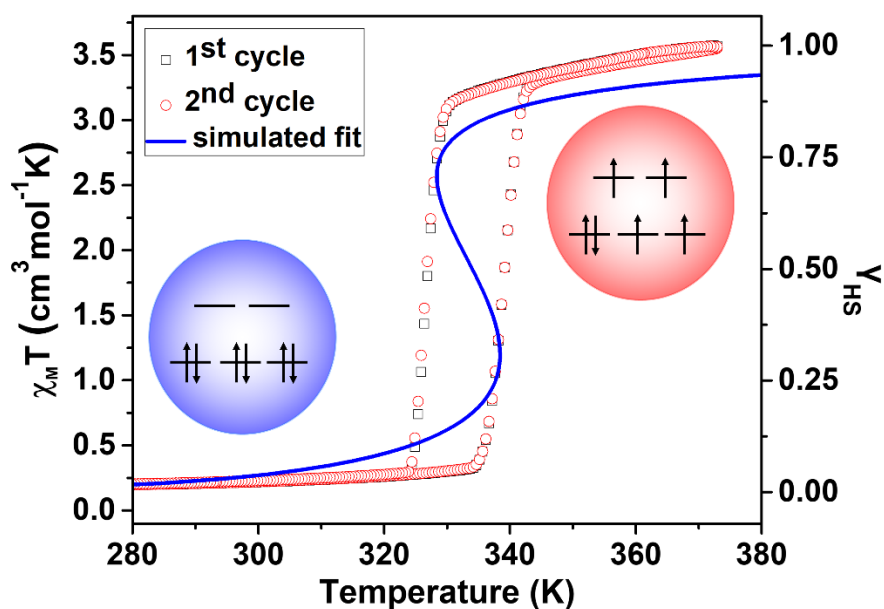
Figure 3. Magnetic properties of $Fe(pz)_2(BH_3CN)_2$ ($\chi_M T$ vs. T plot) recorded in heating and cooling modes at a scan rate of 2 K min^{-1} in two consequent thermal cycles (empty dots) and a simulated curve (blue solid line). The complex displays a cooperative spin transition with a thermal hysteresis of 12 K ($T_{1/2}\uparrow$ = 338 K, $T_{1/2}\downarrow$ = 326 K). A gradual increase of the $\chi_M T$ above 350 K is attributed to a diamagnetic contribution.

Mössbauer spectra of the complex in the two spin states (LS at 293 K and HS at 353 K) demonstrate a complete transition in both directions (Figure 4). At 293 K the spectrum of $Fe(pz)_2(BH_3CN)_2$ shows a unique doublet with an isomer shift of δ^{LS} = 0.327(1) mm s^{-1} and a quadrupole splitting of ΔE_Q^{LS} = 0.458(1) mm s^{-1} in agreement with Fe(II) species in the LS state. When heated to 353 K the spectrum reveals a complete disappearance of the LS species and instead only a doublet typical for the HS state is detected (δ^{HS} = 1.026(1) mm s^{-1} and ΔE_Q^{LS} = 1.356(1) mm s^{-1}).
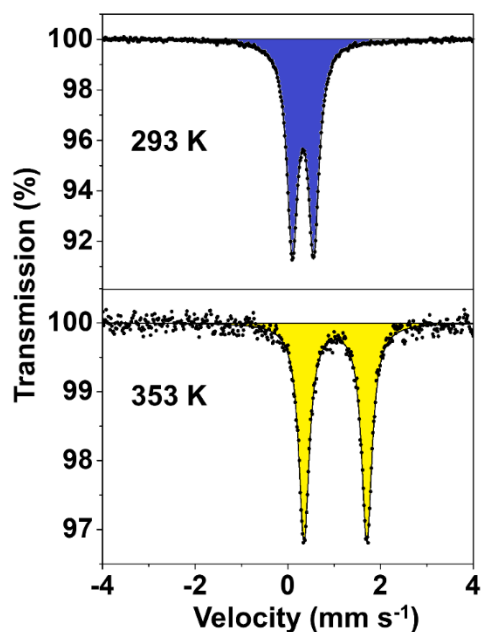
Figure 4. Mössbauer spectra of $Fe(pz)_2(BH_3CN)_2$ at 293 and 353 K reveal a complete transition between diamagnetic and paramagnetic states of all Fe(II) centers.

Optical Measurements. Spin transition is always accompanied by a color change due to the alteration of *d-d* electron transitions in metal ions and charge transfer bands. Therefore, the observed thermochromic effect allows to follow temperature induced spin transitions in complexes by measuring intensity of the transmitted, reflected or scattered light. The title complex has a dark red color in the LS state and orange in the HS state. This is related to the change of the absorption spectra of the complex upon SCO: a band at 530 nm (presumably attributed to the $^1A_1 \rightarrow {}^1T_1$) disappears upon LS→HS transformation while other bands of the charge transfer nature are slightly shifted or not affected (see Figure S3). Optical reflection of $Fe(pz)_2(BH_3CN)_2$ as a function of temperature is shown in Figure 5. The values of transition temperatures obtained in optical experiments are consistent with those, obtained in magnetic measurements: $T_{1/2}\uparrow = 337$ K and $T_{1/2}\downarrow = 321$ K. Independence of the SCO curve profile on the scan rate (in the range 0.5 – 10 K

min^{-1}) is shown in Figure S4 with just very minor changes of the heating branch. This confirms there are no considerable kinetic effects for the transition in this compound. Temperature shift comparing to the magnetic measurements is most likely associated with different thermalization of samples. Optical images of Fe(pz)$_2$(BH$_3$CN)$_2$ powder at 293 K and 363 K are shown in Figure 5b. A drastic color change and an abrupt LS↔HS transition make this complex an attractive thermochromic indicator above RT.
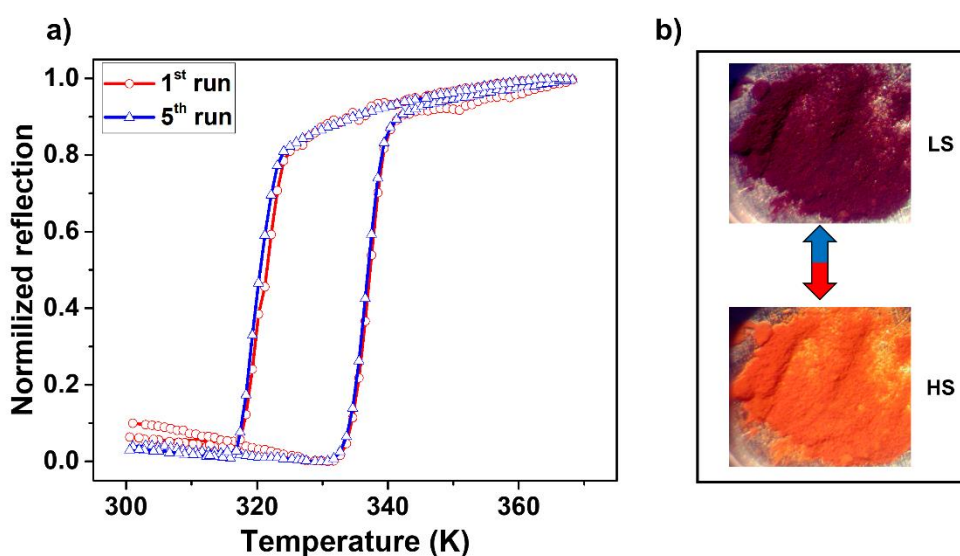

Figure 5. a) Temperature-dependent normalized reflection of Fe(pz)$_2$(BH$_3$CN)$_2$ (heating/cooling rate is 2 K min^{-1}). b) Photographs of Fe(pz)$_2$(BH$_3$CN)$_2$ in different spin states made at 293 K (LS) and 363 K (HS).

The title complex can be processed to composite films with organic polymers using a procedure similar to previously described. Drop-casting of a complex suspension in PMMA/CHCl$_3$ solution leads to free-standing films (Figure 6a). These films were annealed at 95 °C and further used for optical characterization. The PXRD pattern shows no significant changes in the structure of the complex upon composite formation (Figure 6b). However, the changes of some peak intensities

may evidence the preferential orientation of the complex particles in the polymer matrix along *ab* plane. A partial exfoliation may also be supposed.

Elaborated films have colors of the title complex, namely they are dark red at low temperatures (the low-spin form) and orange at high temperatures (the high-spin form). SCO in the composites was monitored in optical reflectance experiments at variable temperatures. The composite films display an abrupt spin transition with thermal hysteresis within the same temperature range as the bulk powder ($T_{1/2}\uparrow$ = 340 K and $T_{1/2}\downarrow$ = 321 K for 20 wt%) (Figure 6c). Such thermochromic behavior makes polymer composites based on $Fe(pz)_2(BH_3CN)_2$ attractive thermochromic material for various sensors and markers. Polymeric composites are also perspective for fabrication of SCO actuators because of the pronounceable expansion occurring upon the spin transition.
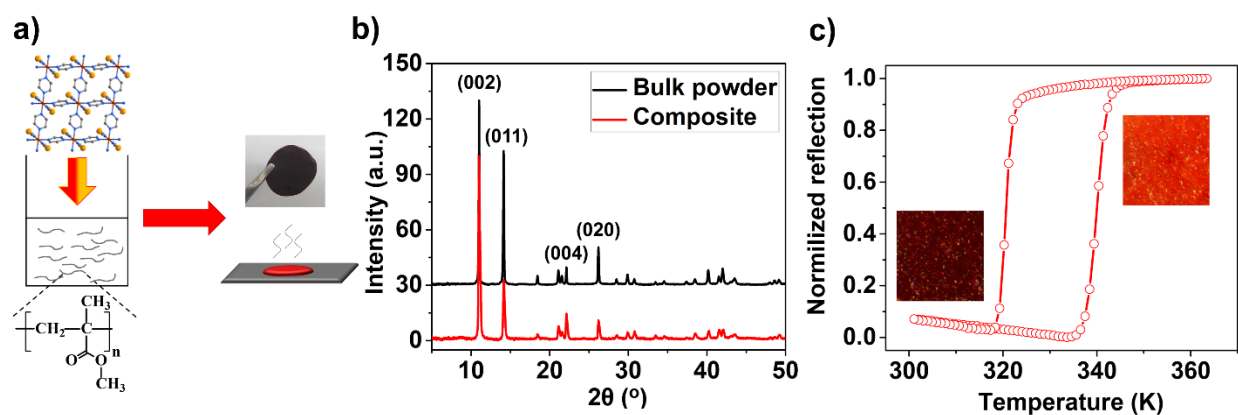

Figure 6. a) Schematic representation of a composite film elaboration; b) PXRD patterns (298 K) of the powder of $Fe(pz)_2(BH_3CN)_2$ and a composite PMMA/SCO film (20 wt%) based on the complex; c) Normalized reflection of $Fe(pz)_2(BH_3CN)_2$-based composite as a function of temperature measured at 2 K min^{-1} scan rate. LS and HS photographs of the film (20 wt%) are inserted.

DSC and TGA characterization. Differential scanning calorimetry (DSC) curves obtained for Fe(pz)$_2$(BH$_3$CN)$_2$ are shown in Figure 7a as the $\Delta C_p(T)$ function. Upon heating an endothermal peak is observed which is associated with the LS→HS transition; the cooling branch has an exothermic peak associated with the HS→LS transition. The obtained critical temperatures (T$_{1/2}$↑ = 338 K and T$_{1/2}$↓ = 322 K) are similar to those obtained in other experiments. Average values of the enthalpy change (ΔH) and the entropy change (ΔS) associated with spin transition, $\Delta H = 19.4$ kJ mol^{-1} and $\Delta S = 58.7$ J mol^{-1} K^{-1}, are consistent with the values typically observed for other cooperative spin transitions[27a,36].
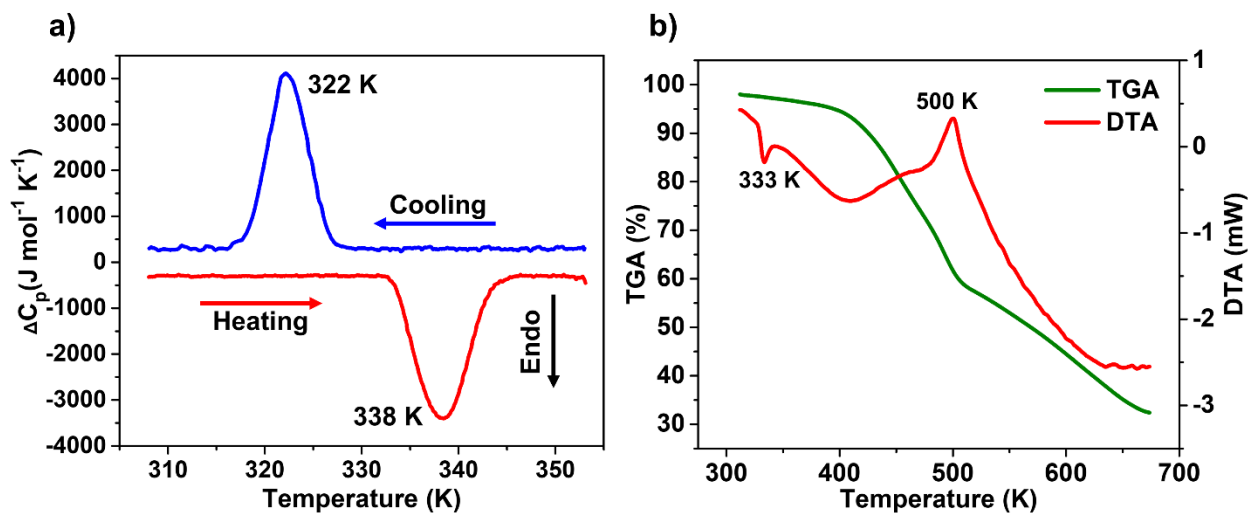

Figure 7. a) DSC curves of Fe(pz)$_2$(BH$_3$CN)$_2$ showing thermal effects upon SCO. Measurements were carried out at 10 K min^{-1} scan rate. b) TGA (green) and DTA (red) curves of Fe(pz)$_2$(BH$_3$CN)$_2$ at 300-673 K in argon flow. A phase transition and a decomposition of the framework are observed.

Thermogravimetric measurements (TGA, Figure 7b) indicate a stability of the framework up to ca. 410 K and a its gradual decomposition above this temperature. Decomposition occurs in a wide range of temperatures and one cannot extract thermal ranges where some distinguished species are

eliminated. Notably, a differential thermal analysis (DTA) curve shows an endothermal peak at ca. 333 K which should be associated with the LS→HS transition.

CONCLUSIONS

Here we reported on a new 2D metal-organic framework displaying cooperative spin crossover above room temperature. Abrupt, complete and reproducible spin transitions occur at 338 K in heating mode and at 326 K in cooling mode, revealing a hysteresis loop of 12 K. Spin transition is accompanied by a striking color change (red ↔ orange), considerable volume change (10.6%), and an attractive operating temperature range. This features, along with a simplicity of the synthesis from commercially available ligands and the stability in the temperature range where switching occurs, make this new complex an attractive material for switchable components of diverse applications, particularly for a fabrication of thermochromic sensors or markers. Notably, a discovery of this complex supports an idea that new practically interesting materials still can be obtained from simple and readily available precursors.

ASSOCIATED CONTENT

Supporting Information.

IR-ATR spectrum of $Fe(pz)_2(BH_3CN)_2$ (Figure S1), experimental and simulated PXRD patterns for $Fe(pz)_2(BH_3CN)_2$ in LS and HS states (Figure S2a,b), absorption spectra recorded in two spin states (Figure S3), temperature scan-rate study of the spin transition in a powder of the complex (Figure S4), crystal data and structure refinement for $Fe(pz)_2(BH_3CN)_2$ at 293 K (Table S1-S4), crystal data and structure refinement for $Fe(pz)_2(BH_3CN)_2$ at 368 K (Table S5-S8), and CIF files. This material is available free of charge via the Internet at http://pubs.acs.org.

AUTHOR INFORMATION

Corresponding Author

*E-mail: illia.guralskyi@univ.kiev.ua.

Author Contributions

The manuscript was written through contributions of all authors. All authors have given approval to the final version of the manuscript.

Notes

The authors declare no competing financial interest.

REFERENCES

(1)   (a) Gütlich, P.; Goodwin, H. A. *Spin Crossover in Transition Metal Compounds*; Springer, 2004; Vol. 233–235. (b) Molnár, G.; Rat, S.; Salmon, L.; Nicolazzi, W.; Bousseksou, A. Spin Crossover Nanomaterials: From Fundamental Concepts to Devices. *Adv. Mater.* **2018**, *30* (5), 1703862. https://doi.org/10.1002/adma.201703862.

(2)   Brooker, S. Spin Crossover with Thermal Hysteresis: Practicalities and Lessons Learnt. *Chem. Soc. Rev.* **2015**, *44* (10), 2880–2892. https://doi.org/10.1039/c4cs00376d.

(3)   (a) Gural'skiy, I. A.; Shylin, S. I.; Golub, B. O.; Ksenofontov, V.; Fritsky, I. O.; Tremel, W. High Temperature Spin Crossover in [Fe(Pyrazine){Ag(CN)$_2$}$_2$] and Its Solvate. *New J. Chem.* **2016**, *40* (11), 9012–9016. https://doi.org/10.1039/C6NJ01472K. (b) Gural'skiy, I. A.; Golub, B. O.; Shylin, S. I.; Ksenofontov, V.; Shepherd, H. J.; Raithby, P. R.; Tremel, W.; Fritsky, I. O. Cooperative High-Temperature Spin Crossover Accompanied by a Highly Anisotropic Structural Distortion. *Eur. J. Inorg. Chem.* **2016**, *2016* (19), 3191–3195. https://doi.org/10.1002/ejic.201600406. (c) Southon, P. D.; Liu, L.; Fellows, E. A.; Price, D. J.; Halder, G. J.; Chapman, K. W.; Moubaraki, B.; Murray, K. S.; Létard, J.-F.; Kepert, C. J. Dynamic Interplay between Spin-Crossover and Host−Guest Function in a Nanoporous Metal−Organic Framework Material. *J. Am. Chem. Soc.* **2009**, *131* (31), 10998–11009. https://doi.org/10.1021/ja902187d. (d) Niel, V.; Martinez-Agudo, J. M.; Muñoz, M. C.; Gaspar, A. B.; Real, J. A. Cooperative Spin Crossover Behavior in Cyanide-Bridged Fe(II)−M(II) Bimetallic 3D Hofmann-like Networks (M = Ni, Pd, and Pt). *Inorg. Chem.* **2001**, *40* (16), 3838–3839. https://doi.org/10.1021/ic010259y. (e) Muñoz, M. C.; Real, J. A. Thermo-, Piezo-, Photo- and Chemo-Switchable Spin Crossover Iron(II)-Metallocyanate Based Coordination Polymers. *Coord. Chem. Rev.* **2011**, *255* (17–18), 2068–2093. https://doi.org/10.1016/j.ccr.2011.02.004.

(4)   Hao, X.; Wei, Y.; Zhang, S. Crystal Structure and Metamagnetic Property of a 2-D Layered Complex, [Fe^{II}(N$_3$)$_2$(Pyz)]$_n$ (Pyz = Pyrazine). *Chem. Commun.* **2000**, *2* (22), 2271–2272. https://doi.org/10.1039/b005137n.

(5)   Wriedt, M.; Jeß, I.; Näther, C. Synthesis, Crystal Structure, and Thermal and Magnetic Properties of New Transition Metal–Pyrazine Coordination Polymers. *Eur. J. Inorg. Chem.* **2009**, *2009* (10), 1406–1413. https://doi.org/10.1002/ejic.200801082.

(6)   Kawamura, A.; Greenwood, A. R.; Filatov, A. S.; Gallagher, A. T.; Galli, G.; Anderson, J. S. Incorporation of Pyrazine and Bipyridine Linkers with High-Spin Fe(II) and Co(II) in a Metal–Organic Framework. *Inorg. Chem.* **2017**, *56* (6), 3349–3356. https://doi.org/10.1021/acs.inorgchem.6b02883.

(7)   (a) Wriedt, M.; Näther, C. Synthesis, Crystal Structures, Thermal and Magnetic Properties of New Selenocyanato Coordination Polymers with Pyrazine as Co-Ligand. *Zeitschrift für Anorg. und Allg. Chemie* **2011**, *637* (6), 666–671. https://doi.org/10.1002/zaac.201000422. (b) Real, J. A.; De Munno, G.; Munoz, M. C.; Julve, M. Crystal Structure and Magnetic Properties of Bis(Isothiocyanato)Bis(Pyrazine)Iron Polymer, a 2D Sheetlike Polymer. *Inorg. Chem.* **1991**, *30* (12), 2701–2704. https://doi.org/10.1021/ic00012a026.

(8)   Chuang, Y.-C.; Liu, C.-T.; Sheu, C.-F.; Ho, W.-L.; Lee, G.-H.; Wang, C.-C.; Wang, Y. New Iron(II) Spin Crossover Coordination Polymers [Fe(μ-Atrz)$_3$]X$_2 \cdot$2H$_2$O (X = ClO$_4^-$, BF$_4^-$) and [Fe(μ-Atrz)(μ-Pyz)(NCS)$_2$]$\cdot$4H$_2$O with an Interesting Solvent Effe. *Inorg. Chem.* **2012**, *51* (8), 4663–4671. https://doi.org/10.1021/ic202626c.

(9)   (a) Yilmaz, V. T.; Senel, E.; Kazak, C. One-Dimensional Pyrazine Bridged M(II)-Saccharinato Coordination Polymers: Synthesis, Characterization, Crystal Structures and Thermal Studies. *Polyhedron* **2007**, *26* (13), 3199–3204. https://doi.org/10.1016/j.poly.2007.02.018. (b) Li, L.; Becker, J. M.; Allan, L. E. N.; Clarkson, G. J.; Turner, S. S.; Scott, P. Structural and Electronic Modulation of Magnetic Properties in a Family of Chiral Iron Coordination Polymers. *Inorg. Chem.* **2011**, *50* (13), 5925–5935. https://doi.org/10.1021/ic102291r. (c) Xia, B.; Zhou, Y.; Wang, Q.-L.; Xu, X.-F.; Tong, Y.-Z.; Bu, X.-H.; Li, J.-R. Photoinduced Electron Transfer and Remarkable Enhancement of Magnetic Susceptibility in Bridging Pyrazine Complexes. *Dalton Trans.*

2018, *47* (44), 15888–15896. https://doi.org/10.1039/C8DT03422B. (d) Kutasi, A. M.; Turner, D. R.; Jensen, P.; Moubaraki, B.; Batten, S. R.; Murray, K. S. Coordination Polymers of Nitrocyanamide, O_2NNCN^-: Synthesis, Structure and Magnetism. *CrystEngComm* **2009**, *11* (10), 2089. https://doi.org/10.1039/b905970a.

(10) (a) Nabei, A.; Kuroda-Sowa, T.; Okubo, T.; Maekawa, M.; Munakata, M. The Effect of Molecular Packing on the Occurrence of Spin Crossover Phenomena in One-Dimensional Fe(II)-Bis-Schiff Base Complexes. *Inorganica Chim. Acta* **2008**, *361* (12–13), 3489–3493. https://doi.org/10.1016/j.ica.2008.02.065. (b) Białońska, A.; Bronisz, R.; Darowska, K.; Drabent, K.; Kusz, J.; Siczek, M.; Weselski, M.; Zubko, M.; Ozarowski, A. Nitrile-Rich Coordination Polymer $^1_\infty\{[Fe(CH_3CN)_4(Pyrazine)](ClO_4)_2\}$ Exhibiting a HS $\leftrightarrows$ LS Transition. *Inorg. Chem.* **2010**, *49* (24), 11267–11269. https://doi.org/10.1021/ic102040y.

(11) Fernandez-Bartolome, E.; Resines-Urien, E.; Murillo-Vidal, M.; Piñeiro-Lopez, L.; Sánchez Costa, J. Sequential Single-Crystal-to-Single-Crystal Vapochromic Inclusion in a Nonporous Coordination Polymer: Unravelling Dynamic Rearrangement for Selective Pyridine Sensing. *Inorg. Chem. Front.* **2021**, *8* (10), 2426–2432. https://doi.org/10.1039/D1QI00059D.

(12) Resines-Urien, E.; Burzurí, E.; Fernandez-Bartolome, E.; García García-Tuñón, M. Á.; de la Presa, P.; Poloni, R.; Teat, S. J.; Costa, J. S. A Switchable Iron-Based Coordination Polymer toward Reversible Acetonitrile Electro-Optical Readout. *Chem. Sci.* **2019**, *10* (27), 6612–6616. https://doi.org/10.1039/C9SC02522G.

(13) (a) Rodríguez-Jiménez, S.; Barltrop, A. S.; White, N. G.; Feltham, H. L. C.; Brooker, S. Solvent Polarity Predictably Tunes Spin Crossover $T_{1/2}$ in Isomeric Iron(II) Pyrimidine Triazoles. *Inorg. Chem.* **2018**, *57* (11), 6266–6282.

https://doi.org/10.1021/acs.inorgchem.8b00128. (b) Rodríguez-Jiménez, S.; Brooker, S. Solid Versus Solution Spin Crossover and the Importance of the Fe–N≡C(X) Angle. *Inorg. Chem.* **2017**, *56* (22), 13697–13708. https://doi.org/10.1021/acs.inorgchem.7b01338. (c) Rodríguez-Jiménez, S.; Yang, M.; Stewart, I.; Garden, A. L.; Brooker, S. A Simple Method of Predicting Spin State in Solution. *J. Am. Chem. Soc.* **2017**, *139* (50), 18392–18396. https://doi.org/10.1021/jacs.7b11069.

(14) (a) Ross, T. M.; Moubaraki, B.; Wallwork, K. S.; Batten, S. R.; Murray, K. S. A Temperature-Dependent Order-Disorder and Crystallographic Phase Transition in a 0D Fe(II) Spin Crossover Compound and Its Non-Spin Crossover Co(II) Isomorph. *Dalton Trans.* **2011**, *40* (39), 10147. https://doi.org/10.1039/c1dt10961h. (b) Scott, H. S.; Ross, T. M.; Batten, S. R.; Gass, I. A.; Moubaraki, B.; Neville, S. M.; Murray, K. S. Iron(II) Mononuclear Materials Containing Functionalised Dipyridylamino-Substituted Triazine Ligands: Structure, Magnetism and Spin Crossover. *Aust. J. Chem.* **2012**, *65* (7), 874. https://doi.org/10.1071/CH12052. (c) Scott, H. S.; Ross, T. M.; Phonsri, W.; Moubaraki, B.; Chastanet, G.; Létard, J.; Batten, S. R.; Murray, K. S. Discrete Fe[II] Spin-Crossover Complexes of 2,2′-Dipyridylamino-Substituted s-Triazine Ligands with Phenoxo, Cyanophenoxo and Dibenzylamino Functionalities. *Eur. J. Inorg. Chem.* **2015**, *2015* (5), 763–777. https://doi.org/10.1002/ejic.201402972.

(15) (a) Ye, Y. S.; Chen, X. Q.; De Cai, Y.; Fei, B.; Dechambenoit, P.; Rouzières, M.; Mathonière, C.; Clérac, R.; Bao, X. Slow Dynamics of the Spin-Crossover Process in an Apparent High-Spin Mononuclear Fe(II) Complex. *Angew. Chem., Int. Ed.* **2019**, *58* (52), 18888–18891. https://doi.org/10.1002/anie.201911538. (b) Liu, X.; Zhou, J.; Bao, X.; Yan, Z.; Peng, G.; Rouzières, M.; Mathonière, C.; Liu, J.-L.; Clérac, R. Mononuclear Fe(II)

Complexes Based on the Methylpyrazinyl-Diamine Ligand: Chemical-, Thermo- and Photocontrol of Their Magnetic Switchability. *Inorg. Chem.* **2017**, *56* (20), 12148–12157. https://doi.org/10.1021/acs.inorgchem.7b01430. (c) Fei, B.; Chen, X. Q.; Cai, Y. De; Fang, J.-K.; Tong, M. L.; Tucek, J.; Bao, X. The Influence of NCE$^-$ (E = S, Se, BH$_3$) Ligands on the Temperature of Spin Crossover in a Family of Iron(II) Mononuclear Complexes. *Inorg. Chem. Front.* **2018**, *5* (7), 1671–1676. https://doi.org/10.1039/C8QI00303C. (d) Zhou, J.; Zhu, B.-W.; Luan, J.; Liu, Z.; Fang, J.-K.; Bao, X.; Peng, G.; Tucek, J.; Bao, S.-S.; Zheng, L.-M. In Air a Spin Crossover Active Iron(II) Complex of Amine/NCBH$_3$$^-$ Ligands Is Converted to a Low Spin Complex of Imine/CN$^-$ Ligands. *Dalton Trans.* **2015**, *44* (47), 20551–20561. https://doi.org/10.1039/C5DT03464G. (e) Chen, X.-Q.; Cai, Y.-D.; Ye, Y.-S.; Tong, M.-L.; Bao, X. Investigation of SCO Property – Structural Relationships in a Family of Mononuclear Fe(II) Complexes. *Inorg. Chem. Front.* **2019**, *6* (8), 2194–2199. https://doi.org/10.1039/C9QI00577C.

(16)   (a) Arroyave, A.; Lennartson, A.; Dragulescu-Andrasi, A.; Pedersen, K. S.; Piligkos, S.; Stoian, S. A.; Greer, S. M.; Pak, C.; Hietsoi, O.; Phan, H.; Hill, S.; McKenzie, C. J.; Shatruk, M. Spin Crossover in Fe(II) Complexes with N$_4$S$_2$ Coordination. *Inorg. Chem.* **2016**, *55* (12), 5904–5913. https://doi.org/10.1021/acs.inorgchem.6b00246. (b) Plaza-Lozano, D.; Conde-Gallardo, A.; Olguín, J. Spin Crossover vs. High-Spin Iron(II) Complexes in N$_4$S$_2$ Coordination Sphere Containing Picolyl-Thioether Ligands and NCE (E=S, Se and BH$_3$) Co-Ligands. *Eur. J. Inorg. Chem.* **2021**, *2021* (28), 2846–2856. https://doi.org/10.1002/ejic.202100355.

(17)   (a) Cuza, E.; Benmansour, S.; Cosquer, N.; Conan, F.; Pillet, S.; Gómez-García, C. J.; Triki, S. Spin Cross-Over (SCO) Anionic Fe(II) Complexes Based on the Tripodal Ligand Tris(2-

Pyridyl)Ethoxymethane. *Magnetochemistry* **2020**, *6* (2), 26. https://doi.org/10.3390/magnetochemistry6020026. (b) Schneider, C. J.; Cashion, J. D.; Chilton, N. F.; Etrillard, C.; Fuentealba, M.; Howard, J. A. K.; Létard, J.; Milsmann, C.; Moubaraki, B.; Sparkes, H. A.; Batten, S. R.; Murray, K. S. Spin Crossover in a 3,5-Bis(2-pyridyl)-1,2,4-triazolate-Bridged Dinuclear Iron(II) Complex [{Fe(NCBH$_3$)(Py)}$_2$(M-L^1)$_2$] – Powder versus Single Crystal Study. *Eur. J. Inorg. Chem.* **2013**, *2013* (5–6), 850–864. https://doi.org/10.1002/ejic.201201075. (c) de Gaetano, Y.; Jeanneau, E.; Verat, A. Y.; Rechignat, L.; Bousseksou, A.; Matouzenko, G. S. Ligand-Induced Distortions and Magneto-Structural Correlations in a Family of Dinuclear Spin Crossover Compounds with Bipyridyl-Like Bridging Ligands. *Eur. J. Inorg. Chem.* **2013**, *2013* (5–6), 1015–1023. https://doi.org/10.1002/ejic.201200711. (d) Klingele, J.; Kaase, D.; Huxel, T.; Gotzmann, C.; Lan, Y. 3-(2-Pyrazyl)-[1,2,4]Triazolo[4,3-a]Pyridine – A Versatile Ligand: Ambidenticity and Coordination Isomerism in Mono- and Polynuclear 3d Transition Metal Complexes. *Polyhedron* **2013**, *52*, 500–514. https://doi.org/10.1016/j.poly.2012.08.043. (e) Gobeze, W. A.; Milway, V. A.; Olguín, J.; Jameson, G. N. L.; Brooker, S. Nine Diiron(II) Complexes of Three Bis-Tetradentate Pyrimidine Based Ligands with NCE (E = S, Se, BH$_3$) Coligands. *Inorg. Chem.* **2012**, *51* (16), 9056–9065. https://doi.org/10.1021/ic3012052.

(18)   (a) Sun, X.-P.; Tang, Z.; Yao, Z.-S.; Tao, J. A Homochiral 3D Framework of Mechanically Interlocked 1D Loops with Solvent-Dependent Spin-State Switching Behaviors. *Chem. Commun.* **2020**, *56* (1), 133–136. https://doi.org/10.1039/C9CC09063K. (b) Sun, X.-P.; Liu, T.; Yao, Z.-S.; Tao, J. Spin Crossover and Photomagnetic Behaviors in One-Dimensional Looped Coordination Polymers. *Dalton Trans.* **2019**, *48* (25), 9243–9249. https://doi.org/10.1039/C9DT01520E. (c) Morita, T.; Nakashima, S.; Yamada, K.; Inoue,

K. Occurrence of the Spin-Crossover Phenomenon of Assembled Complexes, Fe(NCX)$_2$(Bpa)$_2$(X = S, BH$_3$; Bpa = 1,2-Bis(4-Pyridyl)Ethane) by Enclathrating Organic Guest Molecule. *Chem. Lett.* **2006**, *35* (9), 1042–1043. https://doi.org/10.1246/cl.2006.1042. (d) Dote, H.; Kaneko, M.; Inoue, K.; Nakashima, S. Synthesis of Anion-Mixed Crystals of Assembled Complexes Bridged by 1,2-Bis(4-Pyridyl)Ethane and the Ligand Field of Fe(NCS)(NCBH$_3$) Unit. *Bull. Chem. Soc. Jpn.* **2018**, *91* (1), 71–81. https://doi.org/10.1246/bcsj.20170207. (e) Nakashima, S.; Morita, T.; Inoue, K.; Hayami, S. Spiral Assembly of the 1D Chain Sheet of Fe(NCBH$_3$)$_2$(Bpa)$_2$·(Biphenyl) (Bpa = 1,2-Bis(4-Pyridyl)Ethane) and Its Stepwise Spin-Crossover Phenomenon. *Polymers* **2012**, *4* (1), 880–888. https://doi.org/10.3390/polym4010880.

(19)   (a) Xue, J. P.; Wu, W. J.; Li, Q. S.; Yao, Z. S.; Tao, J. A Two-Dimensional Spin-Crossover Coordination Polymer Exhibiting Interlayer Multiple C−H$^{\Delta+}$···H$^{\delta-}$−B Dihydrogen Bonds. *Inorg. Chem.* **2019**, *58* (23), 15705–15709. https://doi.org/10.1021/acs.inorgchem.9b02927. (b) Chen, X.-Y.; Huang, R.-B.; Zheng, L.-S.; Tao, J. Co-Ligand and Solvent Effects on the Spin-Crossover Behaviors of PtS-Type Porous Coordination Polymers. *Inorg. Chem.* **2014**, *53* (10), 5246–5252. https://doi.org/10.1021/ic500463m. (c) Wu, X. R.; Shi, H. Y.; Wei, R. J.; Li, J.; Zheng, L. S.; Tao, J. Coligand and Solvent Effects on the Architectures and Spin-Crossover Properties of (4,4)-Connected Iron(II) Coordination Polymers. *Inorg. Chem.* **2015**, *54* (8), 3773–3780. https://doi.org/10.1021/ic5029542.

(20)   Shin, J. W.; Jeong, A. R.; Jeoung, S.; Moon, H. R.; Komatsumaru, Y.; Hayami, S.; Moon, D.; Min, K. S. Three-Dimensional Iron(II) Porous Coordination Polymer Exhibiting Carbon Dioxide-Dependent Spin Crossover. *Chem. Commun.* **2018**, *54* (34), 4262–4265.

https://doi.org/10.1039/C8CC00678D.

(21)   Scott, H. S.; Ross, T. M.; Chilton, N. F.; Gass, I. A.; Moubaraki, B.; Chastanet, G.; Paradis, N.; Lètard, J.-F.; Vignesh, K. R.; Rajaraman, G.; Batten, S. R.; Murray, K. S. Crown-Linked Dipyridylamino-Triazine Ligands and Their Spin-Crossover Iron(II) Derivatives: Magnetism, Photomagnetism and Cooperativity. *Dalton Trans.* **2013**, *42* (47), 16494. https://doi.org/10.1039/c3dt51839f.

(22)   Coucouvanis, D. *Inorganic Syntheses*; Coucouvanis, D., Ed.; Inorganic Syntheses; John Wiley & Sons, Inc.: New York, USA, 2002; Vol. 33. https://doi.org/10.1002/0471224502.

(23)   (a) Sheldrick, G. M. Crystal Structure Refinement with SHELXL. *Acta Crystallogr. Sect. C Struct. Chem.* **2015**, *71* (1), 3–8. https://doi.org/10.1107/S2053229614024218. (b) Sheldrick, G. M. SHELXT - Integrated Space-Group and Crystal-Structure Determination. *Acta Crystallogr. Sect. A Found. Crystallogr.* **2015**, *71* (1), 3–8. https://doi.org/10.1107/S2053273314026370.

(24)   Dolomanov, O. V.; Bourhis, L. J.; Gildea, R. J.; Howard, J. A. K.; Puschmann, H. OLEX2: A Complete Structure Solution, Refinement and Analysis Program. *J. Appl. Crystallogr.* **2009**, *42* (2), 339–341. https://doi.org/10.1107/S0021889808042726.

(25)   Gütlich, P.; Hauser, A.; Spiering, H. Thermal and Optical Switching of Iron(II) Complexes. *Angew. Chem. Int. Ed. Engl.* **1994**, *33* (20), 2024–2054. https://doi.org/10.1002/anie.199420241.

(26)   Klooster, W. T.; Koetzle, T. F.; Siegbahn, P. E. M.; Richardson, T. B.; Crabtree, R. H. Study of the N−H···H−B Dihydrogen Bond Including the Crystal Structure of BH_3NH_3 by Neutron Diffraction. *J. Am. Chem. Soc.* **1999**, *121* (27), 6337–6343. https://doi.org/10.1021/ja9825332.

(27) (a) Weber, B.; Bauer, W.; Pfaffeneder, T.; Dîrtu, M. M.; Naik, A. D.; Rotaru, A.; Garcia, Y. Influence of Hydrogen Bonding on the Hysteresis Width in Iron(II) Spin-Crossover Complexes. *Eur. J. Inorg. Chem.* **2011**, *2011* (21), 3193–3206. https://doi.org/10.1002/ejic.201100394. (b) Li, N.; Xue, J.-P.; Liu, J.-L.; Wang, Y.-Y.; Yao, Z.-S.; Tao, J. Switchable on–off Spin-Crossover Properties of Iron(<scp>ii</Scp>) Compounds by Trimming Intermolecular Hydrogen Bonds. *Dalton Trans.* **2020**, *49* (4), 998–1001. https://doi.org/10.1039/C9DT04685B.

(28) (a) Hiiuk, V. M.; Shova, S.; Rotaru, A.; Golub, A. A.; Fritsky, I. O.; Gural'Skiy, I. A. Spin Crossover in 2D Iron(II) Phthalazine Cyanometallic Complexes. *Dalton Trans.* **2020**, *49* (16), 5302–5311. https://doi.org/10.1039/d0dt00783h. (b) Dupouy, G.; Marchivie, M.; Triki, S.; Sala-Pala, J.; Salaün, J.-Y.; Gómez-García, C. J.; Guionneau, P. The Key Role of the Intermolecular Π−π Interactions in the Presence of Spin Crossover in Neutral [Fe(Abpt) 2 A 2] Complexes (A = Terminal Monoanion N Ligand). *Inorg. Chem.* **2008**, *47* (19), 8921–8931. https://doi.org/10.1021/ic800955r.

(29) Kroeber, J.; Audiere, J.-P.; Claude, R.; Codjovi, E.; Kahn, O.; Haasnoot, J. G.; Groliere, F.; Jay, C.; Bousseksou, A. Spin Transitions and Thermal Hysteresis in the Molecular-Based Materials [Fe(Htrz)2(Trz)](BF4) and [Fe(Htrz)3](BF4)2.Cntdot.H2O (Htrz = 1,2,4-4H-Triazole; Trz = 1,2,4-Triazolato). *Chem. Mater.* **1994**, *6* (8), 1404–1412. https://doi.org/10.1021/cm00044a044.

(30) (a) Galet, A.; Muñoz, M. C.; Martínez, V.; Real, J. A. Supramolecular Isomerism in Spin Crossover Networks with Aurophilic Interactions. *Chem. Commun.* **2004**, No. 20, 2268–2269. https://doi.org/10.1039/B409974E. (b) Bartual-Murgui, C.; Ortega-Villar, N. A.; Shepherd, H. J.; Muñoz, M. C.; Salmon, L.; Molnár, G.; Bousseksou, A.; Real, J. A.

Enhanced Porosity in a New 3D Hofmann-like Network Exhibiting Humidity Sensitive Cooperative Spin Transitions at Room Temperature. *J. Mater. Chem.* **2011**, *21* (20), 7217. https://doi.org/10.1039/c0jm04387g.

(31)   (a) Grzywa, M.; Röß-Ohlenroth, R.; Muschielok, C.; Oberhofer, H.; Błachowski, A.; Żukrowski, J.; Vieweg, D.; Von Nidda, H. A. K.; Volkmer, D. Cooperative Large-Hysteresis Spin-Crossover Transition in the Iron(II) Triazolate [Fe(Ta)2] Metal-Organic Framework. *Inorg. Chem.* **2020**, *59* (15), 10501–10511. https://doi.org/10.1021/acs.inorgchem.0c00814. (b) Grosjean, A.; Négrier, P.; Bordet, P.; Etrillard, C.; Mondieig, D.; Pechev, S.; Lebraud, E.; Létard, J.; Guionneau, P. Crystal Structures and Spin Crossover in the Polymeric Material [Fe(Htrz) 2 (Trz)](BF 4) Including Coherent-Domain Size Reduction Effects. *Eur. J. Inorg. Chem.* **2013**, *2013* (5–6), 796–802. https://doi.org/10.1002/ejic.201201121.

(32)   Lavrenova, L. G.; Shakirova, O. G. Spin Crossover and Thermochromism of Iron(II) Coordination Compounds with 1,2,4-Triazoles and Tris(Pyrazol-1-yl)Methanes. *Eur. J. Inorg. Chem.* **2013**, *2013* (5–6), 670–682. https://doi.org/10.1002/ejic.201200980.

(33)   Kucheriv, O. I.; Fritsky, I. O.; Gural'skiy, I. A. Spin Crossover in FeII Cyanometallic Frameworks. *Inorganica Chim. Acta* **2021**, *521*, 120303. https://doi.org/10.1016/j.ica.2021.120303.

(34)   Slichter, C. P.; Drickamer, H. G. Pressure-Induced Electronic Changes in Compounds of Iron. *J. Chem. Phys.* **1972**, *56* (5), 2142–2160. https://doi.org/10.1063/1.1677511.

(35)   Kahn, O. *Molecular Magnetism*; Wiley-VCH Verlag GmbH & Co. KGaA: New York/Heidelberg, 1993.

(36)   (a) Piñeiro-López, L.; Valverde-Muñoz, F. J.; Seredyuk, M.; Bartual-Murgui, C.; Muñoz,

M. C.; Real, J. A. Cyanido-Bridged Fe^{II}–M^I Dimetallic Hofmann-Like Spin-Crossover Coordination Polymers Based on 2,6-Naphthyridine. *Eur. J. Inorg. Chem.* **2018**, *2018* (3–4), 289–296. https://doi.org/10.1002/ejic.201700920. (b) Sirenko, V. Y.; Kucheriv, O. I.; Rotaru, A.; Fritsky, I. O.; Gural'skiy, I. A. Direct Synthesis of Spin-Crossover Complexes: An Unexpectedly Revealed New Iron-Triazolic Structure. *Eur. J. Inorg. Chem.* **2020**, *2020* (48), 4523–4531. https://doi.org/https://doi.org/10.1002/ejic.202000848.
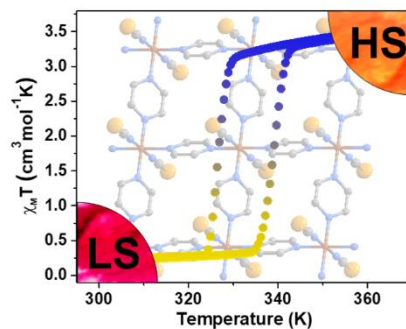
Here we describe a self-assembly of pyrazine and $Fe(BH_3CN)_2$ that afforded a new spin-crossover 2D coordination polymer $[Fe(pyrazine)_2(BH_3CN)_2]_\infty$. It undergoes a complete, abrupt, hysteretic spin transition with $T_{1/2}$ of 338 K (heating) and 326 K (cooling). This transition is accompanied by an increase of the unit cell volume by 10.6%. Simplicity of the synthesis, mild temperatures of transition and other spin transition properties of the new complex make it an attractive material for diverse applications.